Chemical Papers
https://doi.org/10.1007/s11696-021-01653-4

ORIGINAL PAPER

Design, synthesis, and evaluation of metronidazole-1,2,3-triazole derivatives as potent urease inhibitors

Elham Babazadeh Rezaei[1] · Fahimeh Abedinifar[1] · Homa Azizian[2] · Mohammad Nazari Montazer[3] · Mehdi Asadi[3] · Samanesadat Hosseini[4] · Saghi Sepehri[5] · Maryam Mohammadi-Khanaposhtani[6] · Mahmood Biglar[1] · Bagher Larijani[1] · Massoud Amanlou[3] · Mohammad Mahdavi[1]

Received: 9 September 2020 / Accepted: 12 April 2021
© Institute of Chemistry, Slovak Academy of Sciences 2021

Abstract

A new series of metronidazole-1,2,3-triazole derivatives **6a–o** was synthesized and evaluated as *Helicobacter pylori* urease inhibitors. All the synthesized compounds were more potent than standard inhibitor thiourea against urease. Among the synthesized compounds, compound **6f** ($IC_{50} = 1.975 \pm 0.25$ μM) with inhibitory activity around 11-fols more than thiourea ($IC_{50} = 22.00 \pm 0.14$ μM) was the most potent compound. Kinetic study of this compound revealed that compound **6f** inhibited urease in an uncompetitive mode. Based on molecular modeling study, compound **6f** pointed toward the bi-nickel center and stabilized by H-bond and T-shape π–π hydrophobic interactions with the critical residues His492 and Asp633. Moreover, it anchored to the helix-turn-helix motif in the active site cavity through interaction with His593 and Arg609. Consequently, it proposed that compound **6f** through stabilization of active site flap inhibited urease activity.

Keywords Urease inhibitors · 1,2,3-Triazole · Metronidazole · Kinetic study · Molecular modeling

Introduction

Urease is a very potent target in the clinically important complications related to *Helicobacter pylori* (*H. pylori*) (Follmer 2010; Suerbaum and Michetti 2002; Malfertheiner et al. 2017). Urease by providing nitrogen for the growth of *H. pylori*, plays a significant role in the survival of this bacteria (Amtul et al. 2002). *H. pylori* infection is responsible for gastrointestinal diseases such as gastritis, ulceration, gastric carcinomas, and primary gastric lymphomas (Kusters et al. 2006). A very promising strategy for controlling and treating *H. pylori* infection is the use of urease inhibitors (Modolo et al. 2015; Rego et al. 2018; Hameed et al. 2019). Over the last decade, different derivatives of urea, barbituric, thiobarbituric acid, triazole, coumarin, semicarbazone, Schiff bases, and oxadiazoles have been introduced as potent urease inhibitors (Upadhyay 2012; Salar et al. 2019; Arshia et al. 2016; de Fátima et al. 2018; Akhtar et al. 2010; Ullah et al. 2018).

Nitroimidazole scaffold is an attractive pharmacophore for design of biological active compounds with properties such as antimicrobial, antitubercular, and anti-urease (Günay et al. 1999; Kim et al. 2009; Huang et al. 2011). One of the most popular derivatives of nitroimidazole is metronidazole

✉ Mahmood Biglar
Mbiglar@tums.ac.ir

✉ Mohammad Mahdavi
Momahdavi@sina.tums.ac.ir

1 Endocrinology and Metabolism Research Center, Endocrinology and Metabolism Clinical Sciences Institute, Tehran University of Medical Sciences, Tehran, Iran

2 Department of Medicinal Chemistry, School of Pharmacy-International Campus, Iran University of Medical Sciences, Tehran, Iran

3 Department of Medicinal Chemistry, Faculty of Pharmacy and Pharmaceutical Sciences Research Center, Tehran University of Medical Sciences, Tehran, Iran

4 Department of Pharmaceutical Chemistry, School of Pharmacy, Shahid Beheshti University of Medical Sciences, Tehran, Iran

5 Department of Medicinal Chemistry, School of Pharmacy, Ardabil University of Medical Sciences, Ardabil, Iran

6 Cellular and Molecular Biology Research Center, Health Research Institute, Babol University of Medical Sciences, Babol, Iran

Published online: 20 April 2021

that is a potent antibiotic (Finegold 1980). This drug formed of a 2-methyl-5-nitro-1*H*-imidazol moiety and a hydroxyethyl moiety (Fig. 1). Recently, the structure modification in the metronidazole structure especially in alcoholic moiety of this compound has received much attention (Mallia et al. 2005; Mao et al. 2009). For example, metronidazole by a modification in the pendant hydroxyl group converted to urease inhibitors **A** (Fig. 1) (Mao et al. 2009). On the other hand, the 1,2,3-triazole ring has received much attention in medicinal chemistry due to its high dipole moment, capability to form hydrogen bonds, and metabolic stability (Lauria et al. 2014). Given that a valuable method for the construction of the 1,2,3-triazole was reported by Sharp et al., numerous 1,2,3-triazole derivatives with diverse biological effects have been reported (Hou et al. 2012; Lewis et al. 2002; Kharb et al. 2011; H Zhou and Wang 2012; Hoffman et al. 2000; Zhang et al. 2017). Furthermore, recently, our research group has been reported aryl urea-1,2,3-triazole derivatives **B** and 1,2,3-triazole–(thio)barbituric acid derivatives **C** with high inhibitory activity against urease (Fig. 1) (Moghimi et al. 2018; Asgari et al. 2020).

Therefore, in our continuous effort to introduce novel urease inhibitors, we attached 2-methyl-5-nitro-1*H*-imidazole moiety of metronidazole to 1,2,3-triazole derivatives in order to design metronidazole-1,2,3-triazole derivatives **6a–o** as new urease inhibitor (Fig. 1) (Biglar et al. 2020). These compounds were synthesized by click reaction and evaluated against *Jack bean* urease (*JBU*). Furthermore, in silico induced-fit docking of the most active compound was performed to investigate interaction mode, orientation, and conformation of this compound over the active site of *JBU*.

Experimental

All the organic reagents were commercial products from Sigma-Aldrich with the highest purity available (98%) and were used without further purification. Melting points of the synthesized compounds **6a–o** were measured on a Kofler hot stage apparatus and were uncorrected. ^{1}H and ^{13}C NMR spectra of the title compounds were recorded on a Bruker FT-500, using TMS as an internal standard. FT-IR spectra of these compounds were obtained on a Nicolet Magna FTIR 550 spectrophotometer (KBr disks). Mass spectrometry (MS) was done by an Agilent Technology (HP) mass spectrometer performing at ionization potential = 70 eV. The elemental analysis of the compounds **6a–o** for C, H, and N was carried out with an Elementar Analysen system GmbH VarioEL.

General procedure for the synthesis of 2-methyl-5-nitro-1-(prop-2-yn-1-yl)-1*H*-imidazole (3)

A typical process for preparation of 2-methyl-5-nitro-1-(prop-2-yn-1-yl)-1*H*-imidazole; 30 mmol of 2-methyl-5-nitro-1*H*-imidazole, 36 mmol potassium carbonate (1.2 eq) was stirred in DMF (30 mL) at room temperature while 36 mmol propargyl bromide (1.2 eq) was added to the solution dropwise. The reaction completed within 48 h, controlled by thin-layer chromatography (TLC, 50% petroleum ether/50% ethyl acetate). After filtering the solvent to reduce potassium carbonate, the solvent was evaporated, and the residue was washed by hexane to afford 2-methyl-5-nitro-1-(prop-2-yn-1-yl)-1*H*-imidazole.

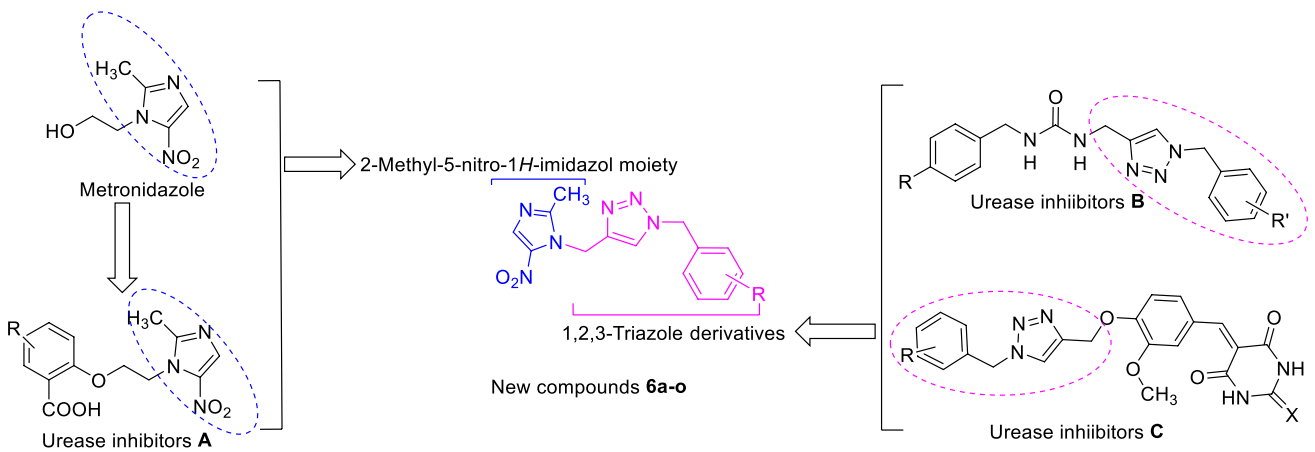

Fig. 1 The design strategy for metronidazole-1,2,3-triazole derivatives **6** as new urease inhibitors

General procedure for the synthesis of 1-benzyl-4-((2-methyl-5-nitro-1*H*-imidazole-1-yl) methyl)-1*H*-1,2,3-triazole derivatives (6a-o)

1-((1-substituted benzyl)-4-((2-methyl-5-nitro-1*H*-imidazole-1-yl)methyl)-1*H*-1,2,3-triazole derivatives **6a–o** were prepared through a click reaction procedure. 1.1 mmol benzyl bromide derivatives, triethylamine (1.1 mmol), and 1.1 mmol sodium azide were stirred at room temperature for 1 h in 5 mL water/tert-butyl alcohol (1:1) as the solvent. Afterward, 0.25 mmol copper sulfate, 0.5 mmol sodium ascorbate, and 1 mmol 2-methyl-5-nitro-1-(prop-2-yn-1-yl)-1*H*-imidazole were added to the solution and pursued by TLC (25% petroleum ether/75% ethyl acetate). After reaction completion through 48 h, water was added to the reaction mixture and filtered. The precipitate was recrystallized in Ethanol to yield **6a–o**.

1-Benzyl-4-((2-methyl-5-nitro-1*H*-imidazol-1-yl) methyl)-1*H*-1,2,3-triazole (6a)

White solid, Yield: 79%, m.p.:144–146 °C. IR (KBr) ν (cm^{-1}): 3300, 3102, 3054, 2951, 1590, 1512, 1440, 1325, 1284, 1215, 1173, 1053, 921, 862, 820, 753, 710, 626. ^{1}H NMR (DMSO-d_6) δ (ppm) (300 MHz): 2.41 (3H, s, CH_3), 5.37 (2H, s, CH_2), 5.62 (2H, s, CH_2-Bn), 7.32–7.42 (5H, m, H 2, H3, H4, H5, H6), 8.25 (1H, s, H-triazole), 8.36(1H, s, H-imidazole). ^{13}C NMR (DMSO-d_6) δ (ppm) (125 MHz): 13.2, 42.0, 53.4, 122.6, 124.4, 128.4, 128.6, 129.2, 136.2, 142.5, 145.5, 145.8. EI-MS *m/z*: 298.10 (Calcd for: $C_{14}H_{14}N_6O_2$: 298.12). Anal. Calcd for $C_{14}H_{14}N_6O_2$: C, 56.37; H, 4.73; N, 28.17; Found C, 56.18; H, 4.72; N, 28.14.

4-((2-Methyl-5-nitro-1*H*-imidazol-1-yl)methyl)-1-(2-methylbenzyl)-1*H*-1,2,3-triazole (6b)

White solid, Yield: 86%, m.p: 147–150 °C. IR (KBr) ν (cm^{-1}): 3381, 3280, 2957, 2327, 2049, 1516, 1448, 1301, 1244, 1178, 1117, 1035, 931, 831, 776, 744. ^{1}H NMR (DMSO-d_6) δ (ppm) (300 MHz): 2.41 (3H, s, CH_3), 5.36 (2H, s, CH_2), 5.63(s, 2H, CH_2–Bn), 7.12(1H, d, J = 7.2 Hz, H3), 7.18–7.26(1H, m, H4,H5,H6), 8.16 (1H, s, H-triazole), 8.36 (1H, s, H-imidazole). ^{13}C NMR (125 MHz, DMSO-d_6), δ ppm: 13.2, 19.0, 42.0, 51.6, 122.6, 124.4, 126.7, 128.9, 129.2, 130.9, 134.3, 136.8, 142.4, 145.5, 145.8. EI-MS *m/z*: 312.10 (Calcd for: $C_{15}H_{16}N_6O_2$: 312.13). Anal. Calcd for $C_{15}H_{16}N_6O_2$: 57.68; H, 5.16; N, 26.91; Found C, 57.38; H, 4.92; N, 26.84.

1-(2-Methoxybenzyl)-4-((2-methyl-5-nitro-1*H*-imidazol-1-yl)methyl)-1*H*-1,2,3-triazole (6c)

White solid, Yield: 86%, m.p.: 126.9–128 °C. IR (KBr) ν (cm^{-1}): 3462, 3381, 3280, 2957, 2327, 2049, 1516, 1448, 1301, 1244, 1178, 1117, 1035, 931, 831, 776, 744. ^{1}H NMR (DMSO-d_6) δ (ppm) (300 MHz): 2.41 (3H, s, CH_3), 3.74 (3H, s, O–C$\underline{H}_3$), 5.37 (2H, s, CH_2), 5.58 (2H, s, CH_2–Bn), 6.86–6.92 (3H, m, H3, H4, H6), 7.27–7.33 (1H, dd,, J = 7.8, 8.7 Hz, H5), 8.25 (1H, s, H-triazole), 8.36 (1H, s, H-imidazole). ^{13}C NMR (125 MHz, DMSO-d_6), δ ppm: 13.2, 42.0, 53.3, 55.5, 114.0, 114.2, 120.5, 122.6, 124.4, 130.4, 137.6, 142.5, 145.5, 145.8, 159.9. Anal. Calcd for $C_{15}H_{16}N_6O_3$: C, 54.87; H, 4.91; N, 25.60; Found C, 54.38; H, 4.92; N, 24.84.

1-(2-Fluorobenzyl)-4-((2-methyl-5-nitro-1*H*-imidazol-1-yl)methyl)-1*H*-1,2,3-triazole (6d)

White solid, Yield: 66%, m.p.: 143–145 °C; IR (KBr) ν (cm^{-1}): 3102, 3067, 2896, 1510, 1420, 1362, 1312, 1289, 1245, 1198, 1126, 1096, 1054, 974, 912, 841, 777, 727, 659. ^{1}H NMR (DMSO-d_6) δ (ppm) (300 MHz): 2.41 (3H, s, CH_3), 5.39 (2H, s, CH_2), 5.80 (2H, s, CH_2–Bn), 7.67–7.73 (1H, dd, J = 7.8, 8.4 Hz, 1H, H5), 7.79 (1H, d, J = 7.8 Hz, H6), 8.20–8.23(2H, m, $^3J_{HF}$ = 9.5 Hz H3,4) 8.34 (1H, s, H-triazole), 8.36 (1H, s, H-imidazole). ^{13}C NMR (125 MHz, DMSO-d_6), δ ppm: 13.2, 42.0, 52.3, 122.6, 123.5, 123.6, 124.7, 130.8, 135.2, 138.3, 142.6, 145.5, 145.8, 148.3. EI-MS *m/z*: 316.10 (Calcd for $C_{14}H_{13}FN_6O_2$: 316.13). Anal. Calcd for $C_{14}H_{13}FN_6O_2$: C, 53.16; H, 4.14; N, 26.57; Found C, 53.38; H, 4.12; N, 26.44.

1-(3-Fluorobenzyl)-4-((2-methyl-5-nitro-1*H*-imidazol-1-yl)methyl)-1*H*-1,2,3-triazole (6e)

White solid, Yield: 85%, m.p: 141.2–146.1 °C. IR (KBr) ν (cm^{-1}): 3112, 3064, 2996, 1510, 1430, 1372, 1322, 1282, 1245, 1197, 1136, 1096, 1054, 974, 912, 841, 777, 727, 659. ^{1}H NMR (DMSO-d_6) δ (ppm) (300 MHz): 2.41 (3H, s, CH_3), 5.38 (2H, s, C$\underline{H}_2$), 5.66 (2H, s, C$\underline{H}_2$–Bn), 7.14–7.21 (3H, m, H2, H4, H6), 7.42–7.48(1H, m, H5), 8.28 (1H, s, H-triazole), 8.36(1H, s, H-imidazole). ^{13}C NMR (125 MHz, DMSO-d_6), δ ppm: 13.2, 42.0, 52.7, 115.2, 115.5(d, $^2J_{C-F}$ = 23 Hz), 115.6, 122.6, 124.5(d, $^4J_{C-F}$ = 5 Hz), 124.6, 131.2 (d, $^3J_{C-F}$ = 14 Hz), 138.8, 138.9, 142.5, 145.5, 145.8, 160.9, 164.2. Anal. Calcd for $C_{14}H_{13}FN_6O_2$: C, 53.16; H, 4.14; N, 26.57; Found C, 53.18; H, 4.13; N, 26.44.

1-(4-Fluorobenzyl)-4-((2-methyl-5-nitro-1*H*-imidazol-1-yl)methyl)-1*H*-1,2,3-triazole (6f)

White solid, Yield: 86%, m.p.: 173–175 °C. IR (KBr) ν (cm^{-1}): 3112, 3064, 2996, 1510, 1430, 1372, 1322, 1282, 1245, 1197, 1136, 1096, 1054, 974, 912, 841, 777, 727, 659. ^{1}H NMR (DMSO-d_6) δ (ppm) (300 MHz): 2.41 (3H, s, CH_3), 5.38 (2H, s, C$\underline{H}_2$), 5.64 (2H, s, C$\underline{H}_2$–Bn), 7.25–7.30 (1H, m, H-aromatic), 7.42–7.43 (3H, m, H-aromatic), 8.29 (1H, s, H-triazole), 8.36 (1H, s, H-imidazole). ^{13}C NMR

(DMSO-d_6) δ (ppm) (125 MHz): 13.2, 42.0, 52.6, 122.6, 124.6, 127.2, 128.4, 128.7, 131.1, 133.7, 138.6, 142.6, 145.5, 145.8. Anal. Calcd for $C_{14}H_{13}FN_6O_2$: C, 53.16; H, 4.14; N, 26.57; Found C, 53.17; H, 4.13; N, 26.54.

1-(2-Chlorobenzyl)-4-((2-methyl-5-nitro-1*H*-imidazol-1-yl)methyl)-1*H*-1,2,3-triazole (6g)

White powder, Yield: 87%, m.p.: 149–152 °C. IR (KBr) ν (cm^{-1}): 3417, 3248, 3102, 3057, 2983, 1590, 1513, 1440, 1330, 1283, 1223, 1174, 1114, 1050, 922, 873, 824, 750, 687. ^{1}H NMR (DMSO-d_6) δ (ppm) (300 MHz): 2.41 (3H, s, CH_3), 5.37 (2H, s, C$\underline{H}_2$), 5.72 (2H, s, C$\underline{H}_2$-Bn), 7.27–7.30(1H, m, H6), 7.36–7.45(2H, m, H4, H5), 7.52–7.55(1H, m, H3), 8. 24(1H, s, H-triazole), 8.35 (1H, s, H-imidazole). ^{13}C NMR (125 MHz, DMSO-d_6), δ ppm: 13.3, 42.0, 51.2, 122.6, 124.8, 128.2, 130.1, 131.1, 133.2, 133.4, 142.3, 145.5, 145.7. EI-MS *m/z*: 332.10 (Calcd for $C_{14}H_{13}ClN_6O_2$: 332.08). Anal. Calcd for $C_{14}H_{13}ClN_6O_2$: C, 50.53; H, 3.94; N, 25.26; Found C, 50.48; H, 3.92; N, 25.24.

1-(3-Chlorobenzyl)-4-((2-methyl-5-nitro-1*H*-imidazol-1-yl)methyl)-1*H*-1,2,3-triazole (6h)

White solid, Yield: 86%, m.p.:126.9–128 °C. IR (KBr) ν (cm^{-1}): 3240, 3002, 2983, 1587, 1510, 1460, 1320, 1283, 1213, 1178, 1114, 1050, 922, 888, 828, 759, 688. ^{1}H NMR (DMSO-d_6) δ (ppm) (300 MHz): 2.41 (3H, s, CH_3), 5.37 (2H, s, C$\underline{H}_2$), 5.61 (2H, s, C$\underline{H}_2$–Bn), 7.19–7.27(2H, m, H4,6), 7.39–7.43(2H, m, H2,5), 8.25 (1H, s, H-triazole), 8.36 (1H, s, H-imidazole). ^{13}C NMR (DMSO-d_6) δ (ppm) (125 MHz): 13.2, 42.0, 52.6, 122.6, 124.6, 127.2, 128.4, 128.6, 131.1, 133.7, 138.6, 142.6, 145.5, 145.8. Anal. Calcd for $C_{14}H_{13}ClN_6O_2$: C, 50.53; H, 3.94; N, 25.26; Found C, 50.51; H, 3.92; N, 25.24.

1-(4-Chlorobenzyl)-4-((2-methyl-5-nitro-1*H*-imidazol-1-yl)methyl)-1*H*-1,2,3-triazole (6i)

White solid, Yield: 74%, m.p.:184.4–185.9 °C. IR (KBr) ν (cm^{-1}): 3248, 3102, 3057, 2983, 1590, 1513, 1440, 1330, 1283, 1223, 1174, 1114, 1050, 922, 873, 824, 750, 687. ^{1}H NMR (DMSO-d_6) δ (ppm) (300 MHz): 2.41 (3H, s, CH_3), 5.37 (2H, s, C$\underline{H}_2$), 5.62 (2H, s, C$\underline{H}_2$–Bn),7.36 (2H, d, J = 8.7 Hz, H2,6), 7.46 (2H, d, J = 8.7 Hz, H3,5), 8.25 (1H, s, H-triazole), 8.36 (1H, s, H-imidazole). ^{13}C NMR (DMSO-d_6) δ (ppm) (125 MHz): 13.2, 42.0, 52.6, 122.6, 124.4, 129.2, 130.4, 133.4, 135.2, 142.5, 145.5, 145.8. Anal. Calcd for $C_{14}H_{13}ClN_6O_2$: C, 50.53; H, 3.94; N, 25.26; Found C, 50.51; H, 3.92; N, 25.24.

1-(2-Bromobenzyl)-4-((2-methyl-5-nitro-1*H*-imidazol-1-yl)methyl)-1*H*-1,2,3-triazole (6j)

White solid, Yield: 82%, m.p.: 141.2–146.1 °C. IR (KBr) ν (cm^{-1}): 3248, 3102, 3057, 2983, 1513, 1440, 1330, 1283, 1223, 1174, 1114, 1050, 922, 873, 824, 750, 687. ^{1}H NMR (DMSO-d_6) δ (ppm) (300 MHz): 2.41 (3H, s, CH_3), 5.38 (2H, s, CH_2), 5.71 (2H, s, CH2-Bn), 7.23 (1H, d, J = 6.6 Hz, H6), 7.30–7.36(1H, dd, J = 7.5 Hz, 7.8 Hz, H4), 7.41–7.45(1H, dd, J = 6.9 Hz, 7.2 Hz, H5), 7.70(1H, d, J = 7.5 Hz, H3), 8.23 (1H, s, H-triazole), 8.36 (1H, s, H-imidazole). ^{13}C NMR (DMSO-d_6) δ (ppm) (125 MHz): 13.3, 42.0, 53.5, 122.6, 123.4, 124.9, 128.7, 130.9, 131.1, 133.4, 135.0, 142.3, 145.5, 145.7. EI-MS *m/z*: 376 (Calcd for $C_{14}H_{13}BrN_6O_2$: 376.03). Anal. Calcd for $C_{14}H_{13}BrN_6O_2$: C, 44.58; H, 3.47; N, 22.28; Found C, 44.48; H, 3.42; N, 22.24.

1-(3-Bromobenzyl)-4-((2-methyl-5-nitro-1*H*-imidazol-1-yl)methyl)-1*H*-1,2,3-triazole (6k)

White solid, Yield: 88%, m.p: 157–160 °C, IR (KBr) ν (cm^{-1}): 3281, 3270, 2967, 2227, 2149, 1536, 1428, 1311, 1254, 1278, 1107, 1235, 936, 837, 786, 734. ^{1}H NMR (DMSO-d_6) δ (ppm) (300 MHz): 2.41 (3H, s, CH_3), 5.37 (2H, s, C$\underline{H}_2$), 5.63 (2H, s, C$\underline{H}_2$-Bn), 7.31–7.39(2H, m, H5,6), 7.54–7.56 (2H, m, H2,4), 8.29 (1H, s, H-triazole), 8.36 (1H, s, H-imidazole). ^{13}C NMR (125 MHz, DMSO-d_6), δ ppm: 13.2, 42.0, 52.5, 122.3, 122.6, 124.6, 127.6, 131.2, 131.4, 131.5, 138.8, 142.6, 145.5, 145.8. Anal. Calcd for $C_{14}H_{13}BrN_6O_2$: C, 44.58; H, 3.47; N, 22.28; Found C, 44.58; H, 3.46; N, 22.27.

1-(4-Bromobenzyl)-4-((2-methyl-5-nitro-1*H*-imidazol-1-yl)methyl)-1*H*-1,2,3-triazole (6l)

White solid, Yield: 81%, m.p: 179–181 °C. IR (KBr) ν (cm^{-1}): 3281, 3270, 2967, 2227, 2149, 1536, 1428, 1311, 1254, 1278, 1107, 1235, 936, 837, 786, 734. ^{1}H NMR (DMSO-d_6) δ (ppm) (300 MHz): 2.41 (3H, s, CH_3), 5.37 (2H, s, C$\underline{H}_2$), 5.61 (2H, s, C$\underline{H}_2$–Bn),7.29 (2H, d, J = 8.4 Hz, H2,6), 7.60 (2H, d, J = 8.4 Hz, H3,5), 8.25(1H, s, H-triazole), 8.36 (1H, s, H-imidazole). ^{13}C NMR (125 MHz, DMSO-d_6), δ ppm: 13.2, 42.0, 52.5, 122.0, 122.6, 124.5, 127.6, 130.7, 132.1, 135.6, 142.5, 145.5, 145.8. Anal. Calcd for $C_{14}H_{13}BrN_6O_2$: C, 44.58; H, 3.47; N, 22.28; Found C, 44.56; H, 3.46; N, 22.28.

4-((2-Methyl-5-nitro-1*H*-imidazol-1-yl)methyl)-1-(2-nitrobenzyl)-1*H*-1,2,3-triazole (6m)

White solid, Yield: 87%, m.p.: 149–152 °C. IR (KBr) ν (cm^{-1}): 3112, 3064, 2996, 1510, 1430, 1372, 1322, 1282, 1245, 1197, 1136, 1096, 1054, 974, 912, 841, 777, 727,

659. ^{1}H NMR (DMSO-d_6) δ (ppm) (300 MHz): 2.42 (3H, s, CH_3), 5.40 (2H, s, CH_2), 5.98 (s, 2H, CH_2–Bn), 7.15 (1H, d, J = 7.8 Hz, H6), 7.63–7.68(1H, dd, J = 7.8, 7.5 Hz, H4), 7.74–7.79 (1H, t, 7.5 Hz, H5), 8.16 (1H, d, J = 8.1 Hz, H3), 8. 27 (1H, s, H-triazole), 8.37 (1H, s, H-imidazole). ^{13}C NMR (125 MHz, DMSO-d_6), δ ppm: 13.2, 42.0, 50.61, 122.6, 125.3, 125.5, 130.2, 130.8, 130.9, 134.8, 142.4, 145.5, 145.8, 148.1. EI-MS *m/z*: 343 (Calcd for $C_{14}H_{13}N_7O_4$: 343.10). Anal. Calcd for $C_{14}H_{13}N_7O_4$: C, 48.98; H, 3.82; N, 28.56; Found C, 48.78; H, 3.82; N, 28.54.

4-((2-Methyl-5-nitro-1*H*-imidazol-1-yl)methyl)-1-(3-nitrobenzyl)-1*H*-1,2,3-triazole (6n)

White solid, Yield: 82%, m.p.: 174.5–176.3 °C. IR (KBr) ν (cm^{-1}): 3112, 3064, 2996, 1510, 1430, 1372, 1322, 1282, 1245, 1197, 1136, 1096, 1054, 974, 912, 841, 777, 727, 659. ^{1}H NMR (DMSO-d_6) δ (ppm) (300 MHz): 2.41 (3H, s, CH_3), 5.39 (2H, s, C$\underline{H}_2$), 5.80 (2H, s, C$\underline{H}_2$–Bn), 7.67–7.73 (1H, dd, J = 7.8, 8.4 Hz, H5), 7.79(1H, d, J = 7.8 Hz, H6), 7.80(1H, s, H2), 8. 22(1H, d, J = 7.2 Hz, H4), 8.34(1H, s, H-triazole), 8.36(1H, s, H-imidazole). ^{13}C NMR (125 MHz, DMSO-d_6), δ ppm: 13.2, 42.0, 52.3, 122.6, 123.3, 123.6, 124.7, 130.8, 135.2, 138.3, 142.6, 145.5, 145.8, 148.3. Anal. Calcd for $C_{14}H_{13}N_7O_4$: C, 48.98; H, 3.82; N, 28.56; Found C, 48.98; H, 3.83; N, 28.54.

4-((2-Methyl-5-nitro-1*H*-imidazol-1-yl)methyl)-1-(4-nitrobenzyl)-1*H*-1,2,3-triazole (6o)

White solid, Yield: 93%, m.p.:185–186 °C. IR (KBr) ν (cm^{-1}): 3366, 3112, 3064, 2996, 1645, 1591, 1510, 1430, 1372, 1322, 1282, 1245, 1197, 1136, 1096, 1054, 974, 912, 841, 777, 727, 659. ^{1}H NMR (DMSO-d_6) δ (ppm) (300 MHz): 2.42 (3H, s, CH_3), 5.39 (2H, s, C$\underline{H}_2$), 5.80 (2H, s, C$\underline{H}_2$–Bn), 7.55 (2H, d, J = 8.7 Hz, H2,6), 8.25, (2H, d, J = 8.7 Hz, H3,5), 8.32 (1H, s, H-triazole), 8.37 (1H, s, H-imidazole). ^{13}C NMR (DMSO-d_6) δ (ppm) (125 MHz): 13.2, 42.0, 52.5, 122.6, 124.4, 124.9, 129.5, 142.6, 143.6, 145.5, 145.8, 147.5. Anal. Calcd for $C_{14}H_{13}N_7O_4$: C, 48.98; H, 3.82; N, 28.56; Found C, 48.88; H, 3.81; N, 28.55.

Urease inhibitory activity

Urease inhibitory activity of the synthesized compounds **6a-o** was evaluated exactly according to our pervious paper (Moghimi et al. 2018). Results are expressed as mean ± SEM (n = 3 experiments).

Kinetic study

To find the type of urease inhibition of the newly synthesized compounds, Lineweaver–Burk plots were applied according to literature (Tan et al. 2017). Urease inhibition mode was determined by varying the concentrations of substrate (urea, 1–4 mM) in the presence of different concentrations of compound **6f** (0, 1, 2, 4 μM) as most potent inhibitor. The inhibitory constant (K_i) was obtained from secondary replotting of Lineweaver–Burk plots. All the experiments were conducted in triplicate.

Molecular modeling

Maestro Molecular Modeling platform (version10.5) by Schrödinger, LLC was performed in order to find out the interactions mode of the most active molecule over urease enzyme active site. The X-ray crystallographic structure of *Jack bean* urease (JBU) (in complex with acetohydroxamic acid, AHA) was downloaded from the Protein Data Bank (PDB ID; 4h9m) (www.rcsb.org). As urease is reported to be functionally active in monomeric state, all the docking studies were performed on single monomer. Also, prosthetic groups and co-factors are not directly involved in urease inhibition, so they removed before docking investigation. Water molecules and co-crystallized ligands were removed from the enzyme crystallographic structure. The 3D structure of the most active synthesized compound was drawn in Marvin 15.10.12.0 program (http://www.chemaxon.com) and converted into pdb file. The Protein Preparation Wizard and the LigPrep module were used to prepare protein and ligand structure properly. The missing side chains of the proteins were filled using the Prime tool, and missing residues were updated.

Induced fit docking (IFD) protocol

The accurate side-chain and backbone flexibility during ligand binding at the active site of urease enzyme was predicted by IFD method using Glide software (Schrödinger LLC 2018, USA). As the kinetic study revealed competitive-type inhibition mechanism against the enzyme, the urease active site was used to generate the grid for IFD calculation. The maximum 20 poses with receptor and ligand van der Waals radii of 0.7 and 0.5, respectively, considered. Residues within 5 Å of the AHA at the active site were refined, followed by side-chain optimization. Structures whose Prime energy is more than 30 kcal/mol are eliminated based on extra precious Glide docking.

Results and discussion

Chemistry

The synthesis of 1-substituted benzyl-4-((2-methyl-5-nitro-1*H*-imidazole-1-yl) methyl)-1*H*-1,2,3-triazole derivatives

6a–o was carried out by the synthetic route outlined in Scheme 1. This procedure was carried out in three steps. The mentioned procedure started of reaction between 2-methyl-5-nitro-1*H*-imidazole **1** and propargyl bromide **2** in the presence of potassium carbonate in DMF to give 2-methyl-5-nitro-1-(prop-2-yn-1-yl)-1H-imidazole **3**. Then, benzyl bromide derivatives **4a–o**, triethylamine, and sodium azide in water/tert-butyl alcohol as solvent reacted at room temperature to give azide derivatives **5a–o**. Finally, sodium ascorbate, copper sulfate, and 2-methyl-5-nitro-1-(prop-2-yn-1-yl)-1*H*-imidazole **3** were added to azide derivatives **5a–o** to afford 1-substituted benzyl-4-((2-methyl-5-nitro-1*H*-imidazole-1-yl)methyl)-1*H*-1,2,3-triazole derivatives **6a–o**.

The structures of target compounds were affirmed by ^{1}H NMR, ^{13}C NMR, and elemental analyses. In the ^{1}H NMR spectra of the title compounds, a singlet at 2.41 reveals the CH_3 group on the imidazole ring. Two singlet peaks in 5.37 ppm and 5.62 ppm are related to CH_2 protons between imidazole and triazole ring, and another is attributed to the benzylic group, respectively. The single proton of triazole moiety appears at 8.25 ppm, and one singlet at 8.30 ppm is considered one proton of the imidazole ring. In the ^{13}C NMR spectra, the typical shifts at 130–132 ppm are related to the triazole ring, which is observed in all spectra.

In vitro inhibition of urease

Metronidazole, the parent molecule **3**, and all the newly synthesized compounds **6a–o** were screened against *H. pylori* urease (Table 1). The obtained results demonstrated that all the synthesized compounds were more potent than standard inhibitor thiourea while metronidazole and compound **3** were inactive against *H. pylori* urease in comparison with thiourea. The most active compounds among the new compounds **6a–o** were compounds **6f**, **6n**, **6m**, and **6c** with substituents 4-fluoro, 3-nitro, 2-nitro, and 2-methoxy on pendant phenyl group attached to 1,2,3-triazole ring (IC_{50} values $\leq 2.712 \pm 0.16$).

The inhibitory activity of metronidazole-1,2,3-triazole derivatives **6a–o** against urease showed that 4-fluoro derivative **6f** (IC_{50} value $= 1.975 \pm 0.25$ µM) was the most potent compound, while 3-chloro and 3-bromo derivatives **6h** and **6k** were less active halogenated derivatives (IC_{50} values $= 6.602 \pm 0.27$–6.336 ± 0.15 µM). As can be seen in Table 1, remaining halogenated derivatives with 2-fluoro, 3-fluoro, 2-chloro, 4-chloro, 2-bromo, and or 4-bromo substituent had good anti-urease activity (IC_{50} values $= 3.30 \pm 0.12$–5.523 ± 0.24 µM) as observed in compounds **6d-e**, **6g**, **6i–j**, and **6l**.

Table 1 The urease inhibitory activity of metronidazole, compound **3**, and the synthesized compounds **6a–o**

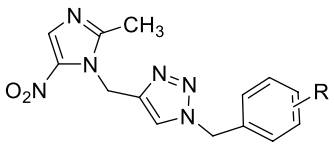

Compound	R	IC_{50} (µM)[a]	Compound	R	IC_{50} (µM)[a]
Metronidazole	–	> 25	**6h**	3-Cl	6.602 ± 0.27
3	–	> 25	**6i**	4-Cl	3.742 ± 0.31
6a	H	4.473 ± 0.17	**6j**	2-Br	5.523 ± 0.24
6b	2-CH_3	9.647 ± 0.21	**6k**	3-Br	6.336 ± 0.15
6c	2-OCH_3	2.712 ± 0.16	**6l**	4-Br	4.017 ± 0.26
6d	2-F	4.395 ± 0.32	**6m**	2-NO_2	2.625 ± 0.09
6e	3-F	3.30 ± 0.12	**6n**	3-NO_2	2.058 ± 0.18
6f	4-F	1.975 ± 0.25	**6o**	4-NO_2	8.069 ± 0.25
6g	2-Cl	4.113 ± 0.11	Thiourea	–	22.00 ± 0.14

[a]Values are the mean ± standard error of mean. All experiments were performed at least three times

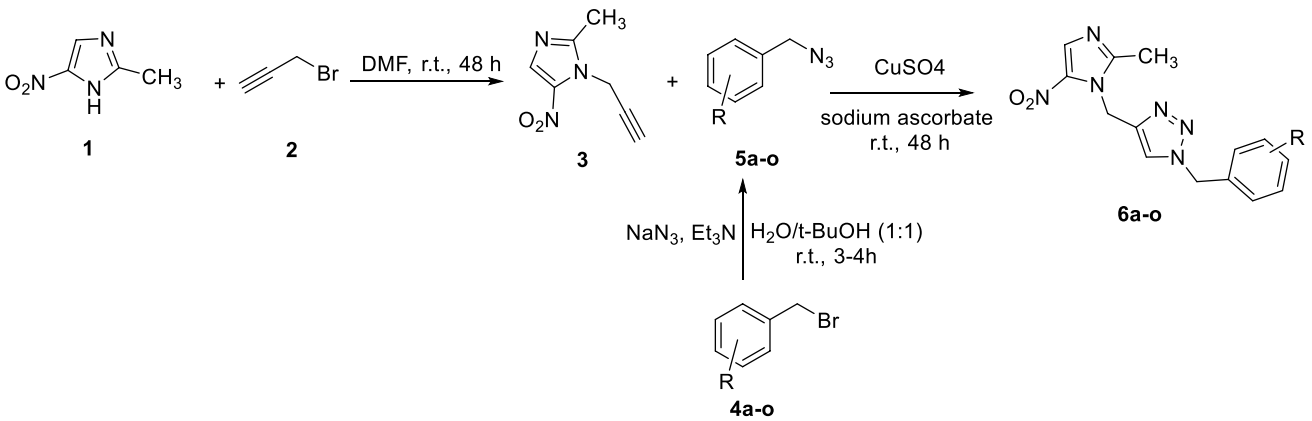

Scheme 1 Synthetic route of the title compounds **6a–o**

The second potent compound among the title synthesized compound was 3-nitro derivative **6n** (IC_{50} value = 2.058 ± 0.18 µM). Changing the position of the nitro group in the pendant phenyl ring from C-3 to C-2, producing compound **6m** (IC_{50} value = 2.625 ± 0.09 µM) slightly diminished the inhibitory activity while movement nitro group of 3-position to 4-position, as in compound **6o** (IC_{50} value = 2.058 ± 0.18 µM), led to a significant decrease in the inhibitory activity.

The fourth most potent compound among the synthesized compounds was 2-methoxy derivative **6c** (IC_{50} value = 2.712 ± 0.16 µM). Replacement of methoxy group of compound **6c** with methyl group, as in compound **6b** (IC_{50} value = 9.647 ± 0.21 µM), decreased inhibitory activity to one-third.

The comparison of anti-urease activity of the metronidazole-1,2,3-triazole derivatives **6** with metronidazole derivatives **A** revealed that new compounds **6** were more active than compounds **A** (Mao et al. 2009). Moreover, as can be seen in Fig. 2, the comparison of IC_{50} values of the newly synthesized metronidazole-1,2,3-triazole derivatives **6** with their corresponding aryl urea-1,2,3-triazole analogs against urease revealed that our new compounds **6** significantly were more potent than their analogs of aryl urea-1,2,3-triazole derivatives **B** (Moghimi et al. 2018).

As can be seen in Fig. 3, our newly synthesized compounds with the exception of 2-methel derivative, were also more potent than their corresponding analogs of 1,2,3-triazole-(thio)barbituric acid derivatives **C** (Asgari et al. 2020).

Kinetic study

To study inhibition mode of the synthesized compounds against urease, the kinetic study was performed on the most active compound **6f**. In this regard, urea was selected as a substrate for urease. As can be seen in Fig. 4a, Lineweaver–Burk plots revealed that compound **6f** inhibited target enzyme urease in an uncompetitive mode because in the presence of this compound both V_{max} and K_m values were decreased. Moreover, the value of K_i (inhibition constant) for compound **6f** was 1.21 ± 0.12 µM (Fig. 4b).

Molecular docking studies

The performed docking procedure was applied based on our previous docking validity study, to evaluate the interaction of the compound **6f** with the best inhibition activity over the urease (*JBU* form) active site in comparison with thiourea as a reference urease inhibitor and metronidazole as a parent molecule for design new compounds **6** (Azizian et al. 2020). Figure 5a–c represents the molecular interactions of the best conformational pose and energy valued docked complex of compound **6f,** thiourea, and metronidazole over the active site of urease.

Figure 5a depicts that the 5-nitro group of compound **6f** tightly coordinated along the metal bi-nickel center and further stabilized by H-bond and electrostatic interactions with His492 and Asp633, respectively, which are belong to the catalytic active site. Also, the 2-methyl-5-nitro-1*H*-imidazole formed π-cation interaction with Arg609. Moreover, the 1,2,3-triazole ring provides several important interactions at the heart of the active site. It provides H-bond and T-shape π–π hydrophobic interaction with Arg609 and His593,

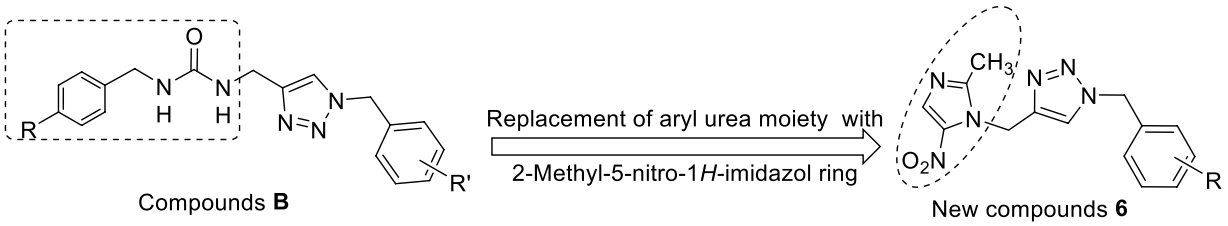

Compounds **B**

R	R'	IC_{50}	R	R'	IC_{50}
H	2-F	149.85 ± 0.12	H	4-Br	184.43 ± 2.16
H	3-F	173.01 ± 1.33	OCH_3	2-F	46.23 ± 0.08
H	4-F	140.91 ± 0.29	OCH_3	3-F	54.26 ± 0.56
H	2-Cl	169.15 ± 2.02	OCH_3	4-F	39.11 ± 1.06
H	3-Cl	192.17 ± 1.20	OCH_3	3-Cl	73.02 ± 0.21
H	4-Cl	161.21 ± 1.52	OCH_3	4-Cl	51.12 ± 1.14

New compounds **6**

R	IC_{50}
2-F	4.395 ± 0.32
3-F	3.30 ± 0.12
4-F	1.975 ± 0.25
2-Cl	4.113 ± 0.11
3-Cl	6.602 ± 0.27
4-Cl	3.742 ± 0.31
4-Br	4.017 ± 0.26

Fig. 2 Comparison between aryl urea-1,2,3-triazole derivatives **B** with new compounds **6**

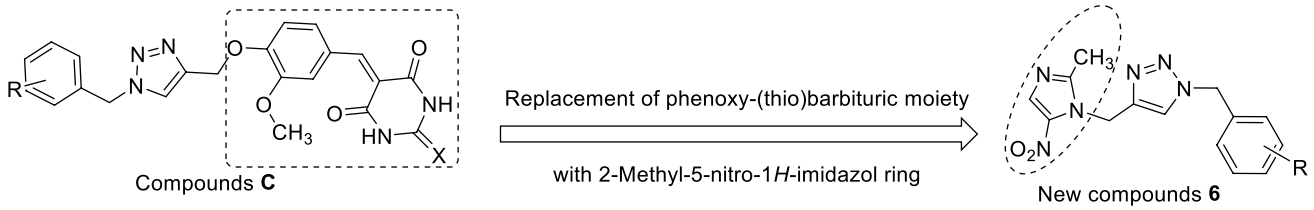

X	R	IC_{50}	X	R	IC_{50}
O	2-CH3	9.32 ± 0.16	O	4-NO_2	24.38 ± 0.22
O	2-F	45.03 ± 0.41	S	2-CH_3	47.96 ± 0.53
O	4-F	16.76 ± 0.25	S	2-F	12.01 ± 0.21
O	2-Cl	10.22 ± 0.13	S	2-Cl	8.10 ± 0.17
O	4-Cl	8.30 ± 0.09	S	4-Cl	25.70 ± 0.32
O	3-Br	14.81 ± 0.15	S	3-Br	76.53 ± 0.46
O	4-Br	13.63 ± 0.24			

R	IC_{50}
2-CH3	9.647 ± 0.21
2-F	4.395 ± 0.32
4-F	1.975 ± 0.25
2-Cl	4.113 ± 0.11
4-Cl	3.742 ± 0.31
3-Br	6.336 ± 0.15
4-Br	4.017 ± 0.26
4-NO_2	8.069 ± 0.25

Fig. 3 Comparison between 1,2,3-triazole–(thio)barbituric acid derivatives **C** with new compounds **6**

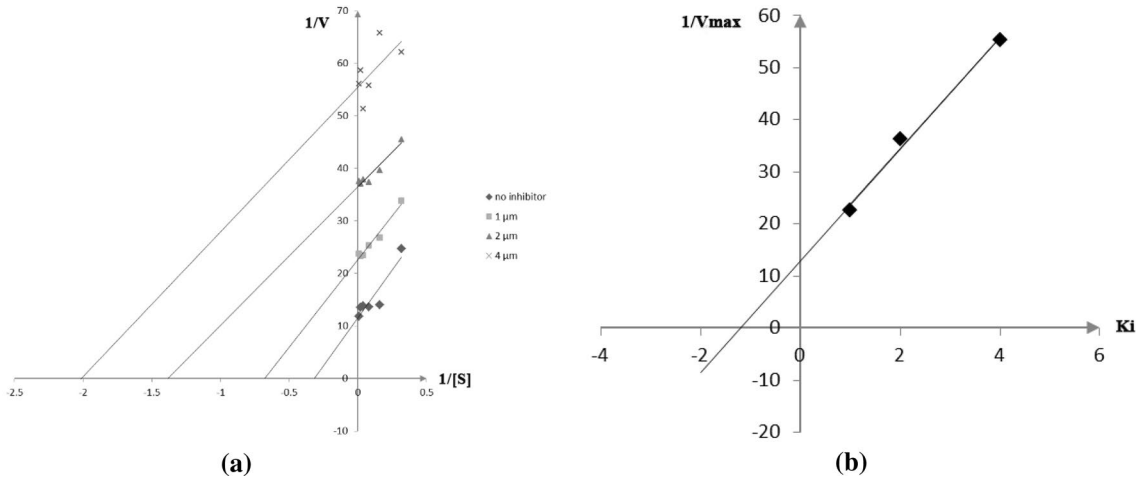

Fig. 4 **a** Lineweaver–Burk plots for the inhibition of urease by compound **6f**; **b** secondary replotting of Lineweaver–Burk plots for determination of K_i value of compound **6f**

respectively, which located at both sides of active site mobile flap and stabilized the compound in front of the mobile flap entrance (represent in a yellow cartoon). In addition, the 1,2,3-triazole ring interacts with His492 and His519 around the bi-nickel center through T-shape π–π hydrophobic. Comparing the bond-state of thiourea (Fig. 5b) revealed only metal coordination, which consequently explains the higher inhibition activity of compound **6f** rather than thiourea.

On the other hand, Fig. 5c depicts the interaction mode of metronidazole as a parent for design of synthesized compounds **6**. The nitro and 2-hydroxyethyl group ligated to the bi-nickel center and interacted with Asp633 and His492 through H-bond and Asp494 by electrostatic interaction. Additionally, metronidazole interacts with Arg609 at one side of the mobile flap through H-bond and electrostatic interactions. Comparison of the interaction mode of compound **6f** and metronidazole reveals that the introduction of the 1,2,3-triazol derivatives instead of 2-hydroxyethyl was responsible for higher inhibition activity of the new synthesized compounds as it not only oriented toward the bi-nickel active site and block deposition of the substrate, but also strongly interacted with the both side of the mobile active site flap which is important for urease inhibition activity. Finally, the consequence of this hybridization is lower binding energy of compound **6f** (glide energy = − 64.56 kcal/mol) in comparison with metronidazole (glide energy = − 34.58 kcal/mol).

Based on crystal structures of the ureases, besides the conserved residues in the active site, including bi-nickel ions, His492, His519, and Asp633, are of the key catalytic

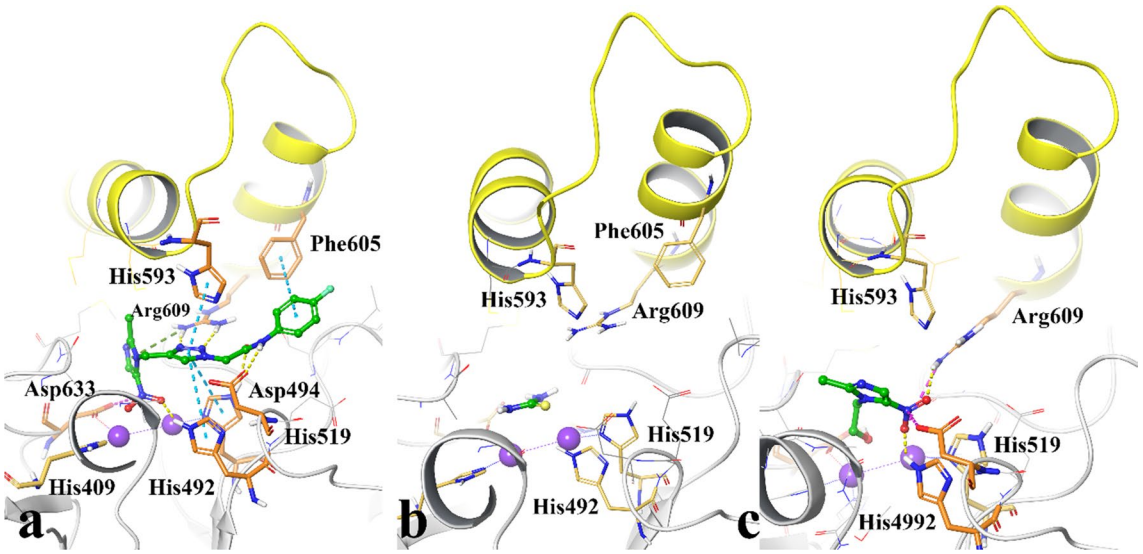

Fig. 5 Docked representation of the synthesized compound **6f** (**a**), thiourea (**b**), and metronidazole (**c**) over the *JBU* active site. The active site flap is colored in yellow. H-bond, π–π stacking, π-cation, and electrostatic interactions are in yellow, blue, green, and pink color, respectively

residues in the urease active site most of the ureases share conserved residues that make up the mobile flap which covers the active site (Balasubramanian and Ponnuraj 2010). In *JBU*, the residues comprising the mobile flap are 590–606 on the α subunit part of the enzyme in a helix-turn-helix motif structure, in which His593 and Arg609 residues belong to each side of active site flap. These residues are the most important residues for urease inhibition because of their role in the flexibility of mobile flap covering the active site entrance, followed by inhibiting the ureolytic activity.

Conclusions

In summary, a new series of metronidazole-1,2,3-triazole derivatives **6a–o** was synthesized and screened as anti-urease agents. These compounds showed excellent inhibitory activity against *H. pylori* urease in comparison with the standard inhibitor thiourea. According to the obtained results, all the newly synthesized compounds **6a–o** with IC_{50} value in range of 1.975 ± 0.25 to 9.647 ± 0.21 µM were more potent than thiourea with IC_{50} value of 22.00 ± 0.14 µM. Among them, compound **6f** depicted the most potent anti-urease activity and is an uncompetitive inhibitor into urease. Compound **6f** interacted with two critical regions over the urease active site: (1) the bi-nickel ions and the related surrounding residues His492, His519, and Asp633 and (2) the conserved residues His593 and Arg609, which belong to the active site flap and are essential for enzyme catalysis. These interactions in addition to preventing catalysis activity at the bi-nickel part led to blocking the flap at the entrance of active site, which significantly reduces the catalytic activity of urease.

Supplementary Information The online version contains supplementary material available at https://doi.org/10.1007/s11696-021-01653-4.

References

Akhtar T, Hameed S, Khan KM, Khan A, Choudhary MI (2010) Design, synthesis, and urease inhibition studies of some 1, 3, 4-oxadiazoles and 1, 2, 4-triazoles derived from mandelic acid. J Enz Inhib Med Chem 25:572–576. https://doi.org/10.3109/14756360903389864

Amtul Z, Siddiqui RA, Choudhary MI (2002) Chemistry and mechanism of urease inhibition. Curr Med Chem 9:1323–1348. https://doi.org/10.2174/0929867023369853

Arshia A, Khan A, Khan KM, Saad SM, Siddiqui NI, Javaid S, Perveen S, Choudhary MI (2016) Synthesis and urease inhibitory activities of benzophenone semicarbazones/thiosemicarbazones. Med Chem Res 25:2666–2679. https://doi.org/10.1007/s00044-016-1673-0

Asgari MS, Azizian H, Nazari Montazer M, Mohammadi-Khanaposhtani M, Asadi M, Sepehri S, Ranjbar PR, Rahimi R, Biglar M, Larijani B, Amanlou M (2020) New 1, 2, 3-triazole–(thio) barbituric acid hybrids as urease inhibitors: design, synthesis, in vitro urease inhibition, docking study, and molecular dynamic simulation. Arch Pharm 353:2000023. https://doi.org/10.1002/ardp.202000023

Azizian H, Esmailnejad A, Vavsari F, Mahernia S, Amanlou M, Balalaie S (2020) Pantoprazole derivatives: synthesis, urease inhibition assay and in silico molecular modeling studies. Chem Select 5:4580–4587. https://doi.org/10.1002/slct.202000578

Balasubramanian A, Ponnuraj K (2010) Crystal structure of the first plant urease from jack bean: 83 years of journey from its first crystal to molecular structure. J Mol Biol 400:274–283. https://doi.org/10.1016/j.jmb.2010.05.009

Biglar M, Mirzazadeh R, Asadi M, Sepehri S, Valizadeh Y, Sarrafi Y, Amanlou M, Larijani B, Mohammadi-Khanaposhtani M, Mahdavi

M (2020) Novel N, N-dimethylbarbituric-pyridinium derivatives as potent urease inhibitors: synthesis, in vitro, and in silico studies. Bioorg Chem 95:103529. https://doi.org/10.1016/j.bioorg.2019.103529

de Fátima Â, de Paula PC, Olímpio CR, de Freitas Oliveira BG, Franco LL, da Silva PH (2018) Schiff bases and their metal complexes as urease inhibitors—a brief review. J Adv Res 13:113–126. https://doi.org/10.1016/j.jare.2018.03.007

Finegold SM (1980) Metronidazole. Ann Intern Med 93:585–587. https://doi.org/10.7326/0003-4819-93-4-585

Follmer C (2010) Ureases as a target for the treatment of gastric and urinary infections. J Clin Pathol 63:424–430. https://doi.org/10.1136/jcp.2009.072595

Günay NS, Çapan G, Ulusoy N, Ergenç N, Ötük G, Kaya D (1999) 5-Nitroimidazole derivatives as possible antibacterial and antifungal agents. Il Farmaco 54:826–831. https://doi.org/10.1016/S0014-827X(99)00109-3

Hameed A, Al-Rashida M, Uroos M, Qazi SU, Naz S, Ishtiaq M, Khan KM (2019) A patent update on therapeutic applications of urease inhibitors (2012–2018). Expert Opin Ther Pat 29:181–189. https://doi.org/10.1080/13543776.2019.1584612

Hoffman HL, Ernst EJ, Klepser ME (2000) Novel triazole antifungal agents. Expert Opin Investig Drugs 9:593–605. https://doi.org/10.1517/13543784.9.3.593

Hou J, Liu X, Shen J, Zhao G, Wang PG (2012) The impact of click chemistry in medicinal chemistry. Expert Opin Drug Discov 7:489–501. https://doi.org/10.1517/17460441.2012.682725

Huang XS, Liu K, Yin Y, Li WM, Ran W, Duan M, Wang LS, Zhu HL (2011) The synthesis, structure and activity evaluation of secnidazole derivatives as Helicobacter pylori urease inhibitors. Curr Bioact Compd 7:268–280. https://doi.org/10.2174/157340711798375868

Kharb R, Sharma PC, Yar MS (2011) Pharmacological significance of triazole scaffold. J Enzyme Inhib Med Chem 26:1–21. https://doi.org/10.3109/14756360903524304

Kim P, Zhang L, Manjunatha UH, Singh R, Patel S, Jiricek J, Keller TH, Boshoff HI, Barry CE III, Dowd CS (2009) Structure-activity relationships of antitubercular nitroimidazoles. 1. Structural features associated with aerobic and anaerobic activities of 4-and 5-nitroimidazoles. J Med Chem 52:1317–1328. https://doi.org/10.1021/jm801246z

Kusters JG, Van Vliet AH, Kuipers EJ (2006) Pathogenesis of Helicobacter pylori infection. Clin Microbiol Rev 19:449–490. https://doi.org/10.1128/CMR.00054-05

Lauria A, Delisi R, Mingoia F, Terenzi A, Martorana A, Barone G, Almerico AM (2014) 1, 2, 3-Triazole in heterocyclic compounds, endowed with biological activity, through 1, 3-dipolar cycloadditions. Eur J Org Chem 2014(16):3289–3306. https://doi.org/10.1002/ejoc.201301695

Lewis WG, Green LG, Grynszpan F, Radić Z, Carlier PR, Taylor P, Finn MG, Sharpless KB (2002) Click chemistry in situ: acetylcholinesterase as a reaction vessel for the selective assembly of a femtomolar inhibitor from an array of building blocks. Angew Chem 114:1095–1099

Malfertheiner P, Megraud F, Omorain CA, Gisbert JP, Kuipers EJ, Axon AT, Bazzoli F, Gasbarrini A, Atherton J, Graham DY, Hunt R (2017) Management of Helicobacter pylori infection—the Maastricht V/Florence consensus report. Gut 66:6–30. https://doi.org/10.1002/1521-3757(20020315)114:6%3c1095::AID-ANGE1095%3e3.0.CO;2-3

Mallia MB, Mathur A, Subramanian S, Banerjee S, Sarma HD, Venkatesh M (2005) A novel [99mTcN] 2+ complex of metronidazole xanthate as a potential agent for targeting hypoxia. Bioorg Med Chem Lett 15:3398–3401. https://doi.org/10.1016/j.bmcl.2005.05.030

Mao WJ, Lv PC, Shi L, Li HQ, Zhu HL (2009) Synthesis, molecular docking and biological evaluation of metronidazole derivatives as potent Helicobacter pylori urease inhibitors. Bioorg Med Chem 17:7531–7536. https://doi.org/10.1016/j.bmc.2009.09.018

Modolo LV, de Souza AX, Horta LP, Araujo DP, de Fatima A (2015) An overview on the potential of natural products as ureases inhibitors: a review. J Adv Res 6:35–44. https://doi.org/10.1016/j.jare.2014.09.001

Moghimi S, Goli-Garmroodi F, Allahyari-Devin M, Pilali H, Hassanzadeh M, Mahernia S, Mahdavi M, Firoozpour L, Amanlou M, Foroumadi A (2018) Synthesis, evaluation, and molecular docking studies of aryl urea-triazole-based derivatives as anti-urease agents. Arch Pharm 351:1800005. https://doi.org/10.1002/ardp.201800005

Rego YF, Queiroz MP, Brito TO, Carvalho PG, de Queiroz VT, de Fátima Â, Macedo F Jr (2018) A review on the development of urease inhibitors as antimicrobial agents against pathogenic bacteria. J Adv Res 13:69–100. https://doi.org/10.1016/j.jare.2018.05.003

Salar U, Nizamani A, Arshad F, Khan KM, Fakhri MI, Perveen S, Ahmed N, Choudhary MI (2019) Bis-coumarins; non-cytotoxic selective urease inhibitors and antiglycation agents. Bioorg Chem 91:103170. https://doi.org/10.1016/j.bioorg.2019.103170

Suerbaum S, Michetti P (2002) Helicobacter pylori infection. N Engl J Med 347:1175–1186. https://doi.org/10.1056/NEJMra020542

Tan L, Li C, Chen H, Mo Z, Zhou J, Liu Y, Ma Z, Xu Y, Yang X, Xie J, Su Z (2017) Epiberberine, a natural protoberberine alkaloid, inhibits urease of Helicobacter pylori and jack bean: susceptibility and mechanism. Eur J Pharm Sci 110:77–86. https://doi.org/10.1016/j.ejps.2017.02.004

Ullah A, Iftikhar F, Arfan M, Kazmi ST, Anjum MN, Haq IU, Ayaz M, Farooq S, Rashid U (2018) Amino acid conjugated antimicrobial drugs: Synthesis, lipophilicity-activity relationship, antibacterial and urease inhibition activity. Eur J Med Chem 145:140–153. https://doi.org/10.1016/j.ejmech.2017.12.089

Upadhyay LSB (2012) Urease inhibitors: a review. Indian J Biotechnol 11:381–388. http://nopr.niscair.res.in/handle/123456789/15679

Zhang S, Xu Z, Gao C, Ren QC, Chang L, Lv ZS, Feng L (2017) Triazole derivatives and their anti-tubercular activity. Eur J Med Chem 138:501–513. https://doi.org/10.1016/j.ejmech.2017.06.051

Zhou CH, Wang Y (2012) Recent researches in triazole compounds as medicinal drugs. Curr Med Chem 19:239–280. https://doi.org/10.2174/092986712803414213

Publisher's Note Springer Nature remains neutral with regard to jurisdictional claims in published maps and institutional affiliations.